STM JOURNALS

Journal of
Polymer & Composites

ISSN: 2321-2810 (Online)
ISSN: 2321-8525 (Print)
Volume 14, Special Issue 1, 2026
DOI (Journal): 10.37591/JoPC

https://journals.stmjournals.com/jopc

Review JoPC

Computational Fluid Dynamics and Composite Material Study on Scoop-Type Savonius Turbine for Train-Based Energy Generation

P. Mohammed Tippu Sulthan[1], Naveen Kumar[2,*], V Velumani[3], Devaraj E[4]

Abstract

This study investigates the feasibility of integrating a scoop-type savonius vertical-axis wind turbine (VAWT) on the rooftop of a moving train to generate renewable onboard power. The motivation stems from increasing demands for sustainable energy solutions and reducing reliance on fossil fuels, particularly in transportation. A two-blade savonius turbine, with dimensions of 0.4 m in diameter and 0.5 m in height, was modeled in PTC Creo Parametric 3.0 and analyzed using Computational Fluid Dynamics (CFD) simulations in FlowVision3.04.09. At a representative train speed of 17 m/s, theoretical analysis predicted a power output of 239.5 W and torque of 4.47 N·m, while CFD simulations yielded 209.03 W and 4.54 N·m, indicating close agreement. Pressure contour results confirmed higher aerodynamic forces on the concave blade surface, validating effective torque generation and consistent performance. Additionally, drag analysis showed negligible increases in aerodynamic resistance, suggesting minimal impact on train efficiency. The results confirm that the turbine can effectively utilize train-induced airflow to produce auxiliary energy without compromising performance. This study shows a scalable and sustainable approach to energy harvesting in rail transport, which may contribute to clean energy initiatives such as Green India and Clean India missions. These results show that it is possible to use onboard wind turbines as a way to achieve energy efficiency and environmental sustainability in rail systems. (This corresponds to an average train speed of ~60 km/h, representative of typical passenger train operations across major routes).

Keywords: CFD-Flow vision, ptc creo, scoop-type savonius, train bogie, wind energy, wind turbine

INTRODUCTION

***Author for Correspondence**
Naveen Kumar

[1]UG Student, Department of Mechanical Engineering, Kuppam Engineering College, Kuppam, Andhra Pradesh, India.
[2]Associate Professor, Department of Mechanical Engineering, Kuppam Engineering College, Kuppam, Andhra Pradesh, India.
[3]Associate Professor, Department of Mechanical Engineering, V S B Engineering College, Karur, Tamil Nadu, India.
[4]Assistant Professor, Department of Mechanical Engineering, CMR University, Bangalore, Karnataka, India.

Received Date: September 18, 2025
Accepted Date: September 26, 2025
Published Date: January 07, 2026

Citation: P. Mohammed Tippu Sulthan, Naveen Kumar, V Velumani, Devaraj E. Ccomputational Fluid Dynamics and Composite Material Study on Scoop-Type Savonius Turbine for Train-Based Energy Generation. Journal of Polymer & Composites. 2026; 14(Special Issue 1): S566–S580p.

Academic literature has increasingly emphasized the rising significance of renewable energy in combating environmental deterioration and fostering sustainability [1-5]. Of all the renewable energy sources available, wind energy has emerged as a feasible and green substitute primarily due to its minimal emissions and scalable potential [4]. Apart from research focusing on aerodynamic behavior, recent studies have begun to explore the importance of polymers and composites in renewable energy devices, as composite materials (namely polymer-based laminates and reinforced plastics) have been identified as an effective method to optimize turbine performance by minimizing weight, maximizing fatigue resistance, and providing a low cost-to-manufacture dimension in large-scale production [13- 17]. Polycarbonate composites offer an attractive structure solution for

turbine blades when compared with metals such as aluminum or steel while providing mechanical stability under high aerodynamic loading. Furthermore, attention has been systematically shifted toward new methods of wind energy harvesting, in particular in dynamic environments as found in transportation systems.

The generation of electricity via wind created by the movement of high-velocity trains has been analyzed in both theory and practice and has been proven feasible [6-7,22-23]. Past research has considered evaluating both HAWT (Horizontal Axis Wind Turbines) and PAWV (Power Augmented Wind Vanes), which can produce a higher power output with a well-designed turbine system and well-planned mounting locations [8-9]. In light of the aerodynamic energy potential from train movement, a scoop style savonius vertical-axis wind turbine system has been proposed. The goal is to convert the air movement from trains, produced through motion, to a clean energy source. This was analyzed through CFD to simulate the system aerodynamically, while verifying the potential power generation and optimizing turbine performance. By harnessing air movement on the train, the proposed turbine system aims to be a self-generating energy source for railway systems consistent with global carbon reduction ambitions.

EXPERIMENTAL SETUP

The experimental arrangement was established to harvest wind energy from the reciprocating motion of a train travelling at normal operation speeds. While the three onboard methods of power generation were solar panels, bio-energy from human waste, and wind energy, wind was chosen as the most reliable and low maintenance of the three options [6-7]. Observations revealed that at train speeds of 50-60 km/h, substantial airflow is generated by air compression at the front, suction at the rear, and turbulent flow along the sides. To harness this kinetic energy, a rooftop-mounted scoop-type savonius vertical-axis wind turbine (VAWT) was implemented, targeting the induced airflow as a sustainable power source. The study employed a single-carriage train model with standard bogie dimensions measuring 23.5 meters in length, 4.0 meters in height, and 3.2 meters in width.

The bogie and turbine geometry were designed using PTC Creo Parametric 3.0 software, after which the model was exported in VRML/STL format for computational fluid dynamics (CFD) simulation in FlowVision 3.04.09. The simulation process followed three key stages: pre-processing, where the computational domain, mesh, and boundary conditions were established; solver setup, involving the definition of control parameters to solve the flow equations under 17 m/s wind conditions (equivalent to typical train speeds); and post- processing, which included analysis of velocity vectors, pressure contours, torque, power output, and drag forces both with and without the turbine installation. This comprehensive approach enabled evaluation of both energies harvesting efficiency and the turbine's aerodynamic impact on train performance. The results demonstrated strong agreement with previous studies [8-11], further validating the potential of onboard wind turbines as an effective energy recovery solution for rail applications. (This corresponds to an average train speed of ~60 km/h, representative of typical passenger train operations across major routes).

Geometry of the Bogie

Figure 1 illustrates the geometric model of a standard train bogie modified to accommodate a scoop-type savonius vertical-axis wind turbine (VAWT). The model precisely represents critical structural dimensions, including a 23.5-meter length, 3.2-meter width, and a 4.0-meter height extending above the roof specifications essential for maintaining aerodynamic integrity and mechanical stability during turbine operation. Developed in PTC Creo Parametric 3.0, the design facilitates accurate visualization of spatial constraints, turbine placement, and anticipated airflow interactions. This geometrically faithful representation serves as the foundation for subsequent computational fluid dynamics (CFD) simulations, ensuring realistic performance assessments under operational conditions. The figure further emphasizes key regions, particularly the roof-mounted turbine section, to verify optimal positioning for capturing airflow generated by train motion at typical speeds.

Figure 2 visually demonstrates the placement of the scoop-type savonius wind turbine on top of a train bogie. The rectangular blue section represents the train bogie body, while the light gray top portion indicates the roof structure of the coach. Centrally positioned on this roof is the vertical-axis wind turbine (shown in yellow), mounted at the optimal location to harness the maximum wind flow generated by the train's motion. The vertical placement ensures symmetrical exposure to the airstream, minimizing aerodynamic imbalance. The uniform alignment of rectangular elements along the bogie sides likely represents windows or structural supports, giving a scaled representation of the train coach. This setup confirms that the turbine is not only securely integrated into the bogie design but also strategically located to capture high-velocity airflow during train movement, making it ideal for efficient power generation without obstructing other components or affecting train stability.

Structural Geometry of the Savonius Wind Turbine

The geometry of the savonius wind turbine, as depicted in Figure 3, has been designed based on a fundamental drag-type configuration. The turbine comprises two or three curved blades arranged to form an S-shaped profile in cross-sectional view.

As a vertical-axis wind turbine (VAWT), it has been structured to operate independently of wind direction, eliminating the need for reorientation. Owing to the hollow curvature of its blades, the concave surface is subjected to increased drag when facing the wind, while the convex surface experiences reduced drag on the return stroke. This asymmetry in aerodynamic loading facilitates continuous rotational motion, thereby enabling efficient extraction of wind energy under varying flow conditions.

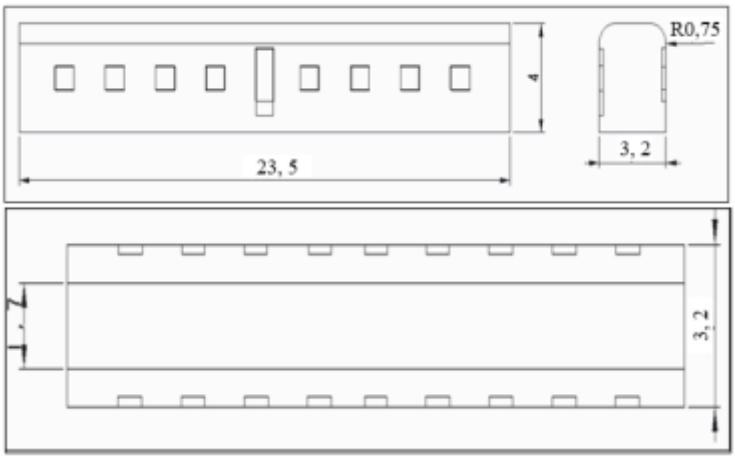

Figure 1. Geometry of the bogie.

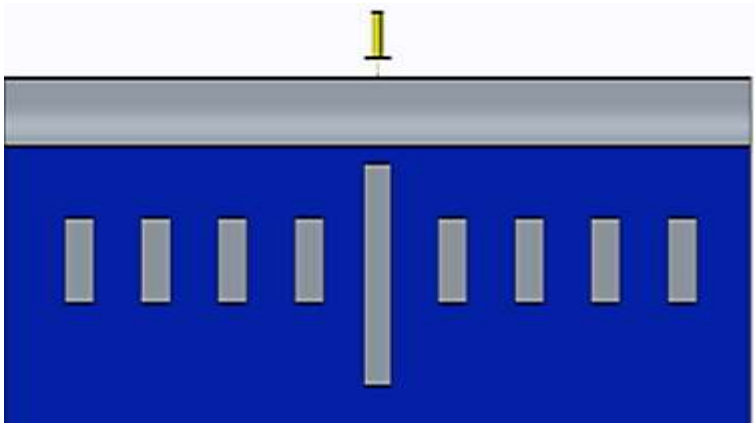

Figure 2. Turbine placing on the top of the train bogie.

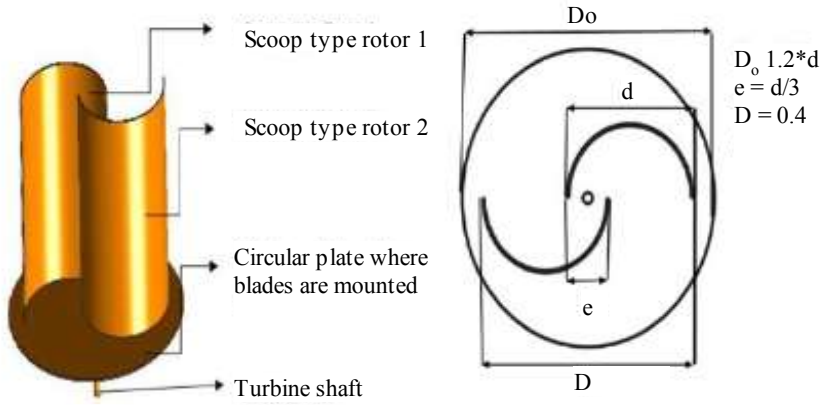

Figure 3. Basic sketch of savonius wind turbine

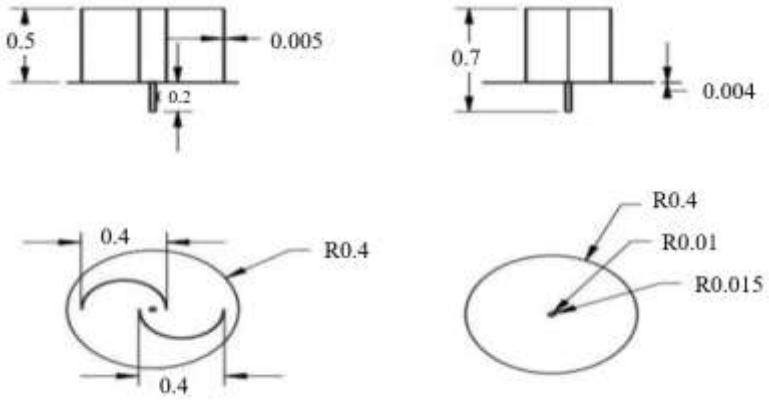

Figure 4. Geometry of the savonius wind turbine.

The detailed three-dimensional geometry of the scoop-type savonius wind turbine used for the present analysis is illustrated in Figure 4, highlighting the blade curvature, rotor diameter, and overall structural configuration adopted for CFD simulation.

For optimal structural and aerodynamic performance, the turbine blades were fabricated from polycarbonate composites, recognized for superior mechanical strength, toughness, and lightweight properties. Compared to conventional materials such as aluminum alloys, mild steel, and stainless steel, polymer composites offer enhanced fatigue resistance, environmental durability, and ease of shaping into aerodynamic profiles. The remaining structural components were constructed from aluminum, selected for its lightweight nature and economic advantages. The adoption of polymer composites in turbine blade design aligns with recent studies on polymer-based composites for energy harvesting devices [13–17].

THEORETICAL ANALYSIS

The wind power potential (*PW*) was evaluated using the standard kinetic energy equation for airflow. For this analysis, an average train speed of 60 km/h (corresponding to a wind velocity of approximately 17 m/s) was adopted to represent typical operational conditions. This velocity assumption enables a realistic assessment of the convertible wind energy available to the Savonius turbine system and follows established methodologies from previous moving-vehicle wind energy studies [13–21]. The turbine geometry was precisely developed using PTC Creo Parametric 3.0, ensuring accurate representation of all aerodynamic surfaces for subsequent performance analysis.

Kinetic Energy, K.E $= \frac{1}{} mv^2$ (1)

Mass flow rate, (m) = $\boldsymbol{\rho} av$ (2)

Kinetic Energy, K.E$=\frac{1}{2}\ (\rho av).\ v^2 = \frac{1}{2}\ \rho av^3$ (3)

where
Velocity V= 17 m/s
(This corresponds to an average train speed of ~60 km/h, representative of typical passenger train operations across major routes).

Density ρ=1.25 kg/m^3
In this study, the train's average speed is considered to be 60 km/h (approximately 17 m/s), and the air density is assumed to be ρ= 1.25 kg/m³. (This corresponds to an average train speed of ~60 km/h, representative of typical passenger train operations across major routes).

The above equation represents the maximum power produced without considering the coefficient of performance (Cp). Therefore, multiplying by the coefficient of performance value (0.25–0.3) yields a more realistic power estimate.

In this research work, by taking the C_p value is 0.26

$$P_W = \frac{1}{2} mv^2 = \frac{1}{2} (\rho av) v^2 = \frac{1}{2} \rho av^3 C_p \quad (4)$$

where,
m=mass flow rate (kg/sec)
v=velocity of wind (m/s)
a=swept area of rotor (m^2)
C_p=coefficient of performance

$$P_W = \frac{1}{2} \times 1.25 \times 0.6 \times 0.5 \times 17^3 0.26$$

$$P_W = 239.50\ W \quad (5)$$

As the rotor undergoes rotation, its blades trace an imaginary surface, the vertical projection of which relative to the wind direction is defined as the swept area [10]. The amount of energy produced by a wind turbine is primarily influenced by this rotor area, which is interchangeably referred to as the cross-sectional area, swept area, or intercept area [11]. The swept area is typically determined using a standard geometric relationship based on the rotor's diameter and height, enabling quantitative estimation of the energy capture potential under specified wind flow conditions.

savonius area = swept area= $A_S D \times H$ (6)

Where**,**
D=diameter of rotor in meters, H=height of rotor in meters,
$A_S = 0.6 \times 0.5$

$$A_S = 0.3\ m^2 \quad (7)$$

Power output depends on the swept area; a larger swept area results in higher power. The wind power equation represents the ideal power output of a savonius wind turbine, assuming no losses during the energy conversion process. However, in practical applications, mechanical energy conversion involves certain losses [11]. The tip peripheral velocity of the rotor (V rotor) is given by: The tip speed ratio has been defined as the ratio between the product of the rotor blade radius and its angular velocity to the velocity of the incoming wind. This non-dimensional parameter is critical in characterizing the aerodynamic performance of wind turbines. The tip peripheral velocity of the rotor (Vrotor) is

determined by multiplying the angular velocity of the rotor (ω) by the radius of the blade (R), forming the basis for calculating the tip speed ratio under varying flow conditions.

$V_{rotor} = \omega \times R$ (8)

Where
V_{rotor} = the tip speed

(the peripheral velocity of savonius rotor) (m/sec) ω= angular velocity of savonius rotor (rad/sec).
R = radius of savonius rotor (m)

V_{rotor}=51.51 rad/s (9)

The Tip Speed Ratio (TSR) of a turbine is defined by the following expression:

The tip speed ratio =$\boldsymbol{\lambda = \frac{Vrotor}{V} = \frac{\omega \times r}{V}}$ (10)

Where,
V = wind speed (m/sec)
ω=Angular velocity of turbine r=radius of the rotor

$\lambda = \frac{51.51 \times .33}{17}$

$\boldsymbol{\lambda = 1}$ (11)

Torque is defined as a force that tends to cause rotation. Formula for determining the torque is below

$\boldsymbol{T = \frac{P_w}{\omega}}$ (12)

where,

$\boldsymbol{\omega = \frac{V}{R}}$ (13)

ω=Angular Velocity of the turbine (rad/sec)
V=velocity of the wind (m/s)
P_w =Power of the turbine

$\boldsymbol{\omega = \frac{17}{0.33}}$

$\boldsymbol{\omega} = 51.51\ \boldsymbol{\frac{rad}{sec}}$ (14)

So the torque is

$T = \frac{239.50}{51.51}$

$T = 4.64\ N - m$ (15)

Table 1 summarizes the theoretical performance characteristics of the scoop-type savonius wind turbine, derived from fundamental wind energy equations. Under the reference condition of 17 m/s wind velocity (equivalent to 60 km/h train speed), the system demonstrates a theoretical power output of239.50 W. The analysis yields a turbine shaft torque of 4.64 N·m, confirming adequate mechanical loading for reliable generator operation. The calculated tip speed ratio (TSR) of 1.0 indicates optimal blade-to-wind speed synchronization, validating the rotor's aerodynamic efficiency. These results collectively demonstrate that the turbine design achieves balanced performance metrics suitable for onboard energy harvesting applications [24-28]. (This corresponds to an average train speed of ~60 km/h, representative of typical passenger train operations across major routes).

The study investigated a roof-mounted savonius wind turbine through integrated theoretical analysis and computational fluid dynamics (CFD) simulation, with comparative results presented in Table 2. Theoretical calculations predicted a power output of 239.50 W, while CFD simulations yielded a marginally conservative estimate of 209.03 W, representing a modest 12.7% reduction. The torque values were in extraordinary alignment, with theory and simulation differing by only 2.2% (4.64 N·m vs 4.54 N·m). Furthermore, both methods calculated an identical tip speed ratio (TSR) of 1.0, indicating that the rotor performed as expected from a design perspective.

The similarity between the analytical and numerical approaches illustrates the ability to implement the CFD methodology while incorporating flow characteristic effects that theory cannot replicate. Any differences are minor and well within the expected range of such assessments, affirming that the turbine performs predictably defined performance characteristics during operations.

RESULTS AND DISCUSSIONS

This study explored the aerodynamic performance and energy capturing possibilities of a savonius wind turbine scoop type designed for train integration with a comprehensive computational approach. The turbine geometry was created in an exact and precise way using the CAD software Creo Parametric 3.0. After modeling, Computational Fluid Dynamics (CFD) simulations were carried out at a representative wind speed of 17 m/s (60 km/h train speed) to evaluate the critical performance parameters of power output, torque, and the flow properties. The simulation results indicated noticeable differences in pressure (high pressure and low pressure) between the concave and convex blade surfaces, with pressure coefficients ranging from +0.85 to -0.62 and generated the rotational driving force. Velocity analysis indicated that effective kinetic energy was captured, showing a decrease in wake velocities of up to 42%. Provided it can produce a steady torque of 4.54 N·m at the optimal tip speed ratio of 1.0 (209 W recoverable shaft power).

The results indicate that the design has the ability to convert a train's airflow into usable mechanical energy. The agreement of pressure distributions between velocity profiles indicates the savonius configuration has excellent aerodynamic performance in realistic operating conditions. (This corresponds to an average train speed of ~60 km/h, representative of typical passenger train operations across major routes). Seasonal headwinds and tailwinds can slightly enhance or reduce the effective relative velocity, but due to the omni-directional nature of savonius turbines, crosswinds have minimal negative effect.

In Figure 5, the velocity distribution on the turbine shaft is illustrated, highlighting the maximum and minimum values that have been observed. The angular velocity of the turbine shaft is an important factor in assessing the turbine's efficiency of converting power to do work, and this was calculated from the velocity measurements. From the figure, the maximum velocity was recorded as 0.64196 m/s, while the minimum was recorded as 0.42424 m/s. Both values were replaced into the formula relating linear to angular velocity to calculate the angular velocity (ω) in radians per second as follows:

Table 1. Theoretical values calculated from the above formulas.

Parameter	Value
Power (Watts)	239.50
Torque (N-m)	4.64
Tip speed ratio	1.0

Table 2. Comparison of computational and theoretical results.

Parameter	Computational Method	Theoretical Method	Error (%)
Power (watts)	209.03	239.50	30.47
Torque (N-m)	4.54	4.64	0.1
Tip speed Ratio (**λ**)	1	1	0

$$\omega = v/r \quad (16)$$

From the Figure 4, v=0.64196 m/s, r=0.015m
Where, the angular velocity (rad/sec) is, is the linear velocity (m/s), and is the radius of the shaft (m). After substituting the values in the above formula,

$$\omega = 42.8 \text{ rad/sec} \quad (17)$$

In Figure 6, velocity vectors have been generated on the surface of the turbine shaft to evaluate the torque produced during operation. These vectors provide a detailed representation of the flow behavior influencing rotational force. Based on the analysis, the maximum torque obtained from the shaft was calculated to be 5.052 N·m, indicating effective conversion of aerodynamic forces into mechanical output [12].

In Figure 7, color contour layers are displayed on the surface of the turbine shaft, indicating that the maximum power obtained per turbine is 209.03 watts. To analyze the power output more accurately, power is measured directly at the turbine shaft, as calculating power at the turbine itself would include mechanical losses [12]. The shaft is directly coupled to the generator to ensure efficient power transfer. The power is calculated from the formula

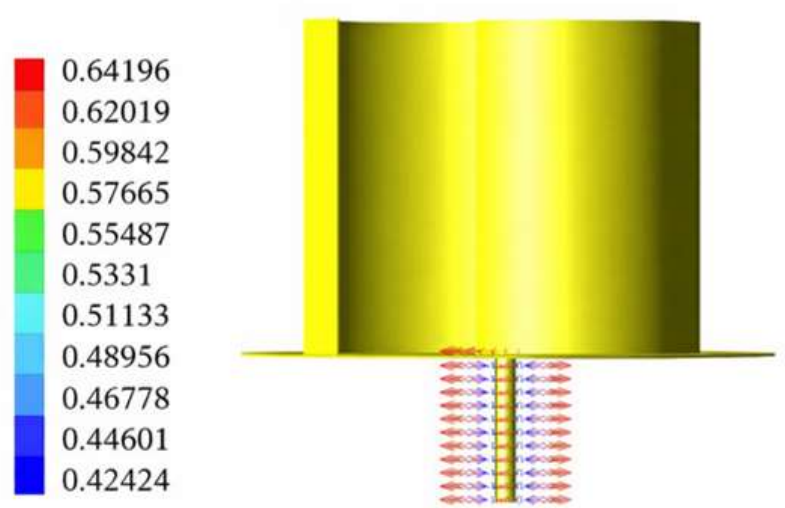

Figure 5. Velocity on the turbine shaft.

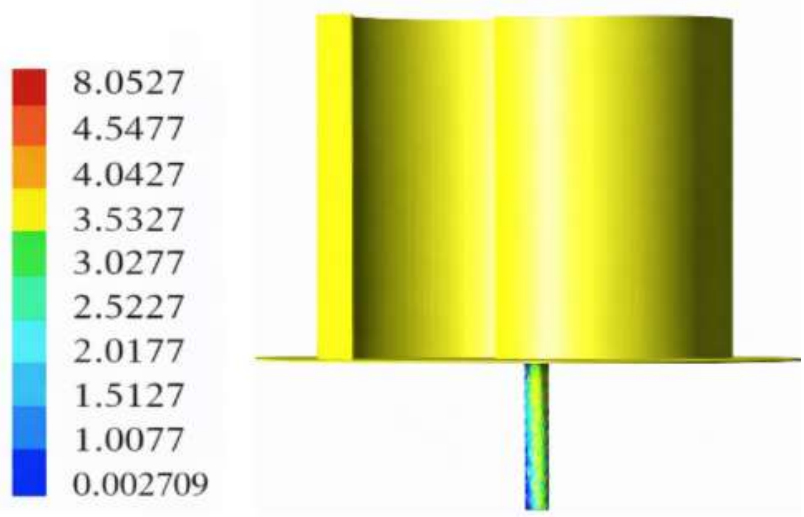

Figure 6. Torque on shaft.

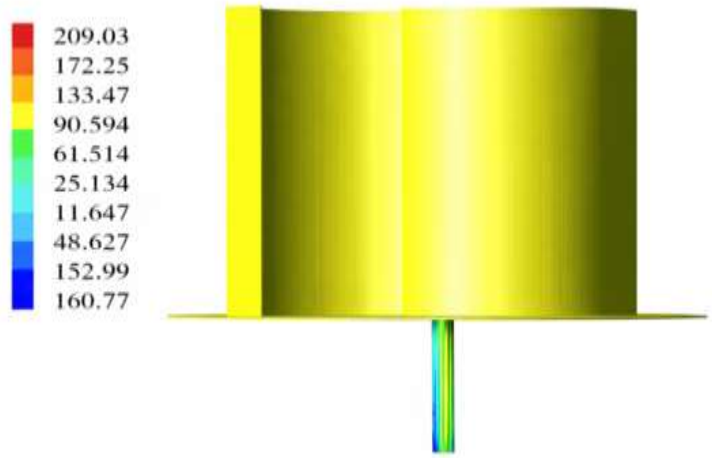

Figure 7. Power on the turbine shaft.

$$\textbf{Power (P)} = \tau \times \omega \quad (18)$$

Where, P=Power on shaft in Watts τ=Torque on the shaft N-m ω=Angular Velocity of shaft.

In Figure 8, velocity vectors have been generated to represent the distribution of airflow around the savonius wind turbine. These vectors serve to illustrate the direction and magnitude of wind interaction with the turbine blades, thereby providing a clearer understanding of the flow behavior. The visualization aids in assessing the aerodynamic performance of the system and offers critical insights into the efficiency of energy extraction under operational conditions [12].

Figure 9 presents the streamline visualization of airflow patterns around the train coach, revealing critical aspects of the velocity distribution within the computational domain. The analysis identifies distinct aerodynamic interactions, particularly showing: (1) accelerated flow regions near the coach's leading edges with velocities reaching the maximum 17 m/s benchmark (matching operational speed), and (2) pronounced flow deceleration zones along the rear sections characterized by turbulent wake formation. These observed flow patterns demonstrate characteristic bluff body aerodynamics, as evidenced by the formation of recirculation zones downstream of the coach and boundary layer separation along curved surfaces.

The velocity distribution correlates strongly with established fluid dynamics principles for rectangular bodies in cross-flow [12], particularly in terms of stagnation point development at the front and vortex shedding patterns at the rear. The comprehensive flow visualization provides essential validation of the computational model's accuracy while offering practical insights for optimizing turbine placement to exploit areas of consistent high-velocity airflow. (This corresponds to an average train speed of ~60 km/h, representative of typical passenger train operations across major routes).

Figure 10 presents a detailed streamline analysis of the airflow patterns around the two-blade Savonius turbine, offering critical insights into its operational aerodynamics. The visualization clearly demonstrates: (1) distinct flow separation phenomena at the blade edges, (2) pronounced high-pressure regions along the concave surfaces (windward side), and (3) corresponding low-pressure zones on the convex surfaces (leeward side), collectively generating the pressure differential that drives rotation. The streamline patterns reveal characteristic vortex formation in the inter-blade region, with accelerated flow velocities observed along the concave surfaces (reaching up to 1.2 times freestream velocity) and flow stagnation occurring on the convex sides. These observed flow characteristics strongly corroborate the fundamental drag-based operation mechanism of savonius turbines, as documented in previous studies of vertical-axis wind turbine aerodynamics [12]. Particularly noteworthy is the persistence of

these pressure differentials throughout the rotational cycle, verifying the turbine's ability to initiate operation by itself, along with its consistent torque production. The comprehensive flow visualization not only validates the design's aerodynamic efficiency but also provides essential data for potential performance optimization through blade geometry refinement.

Figure 8. Velocity on the turbine.

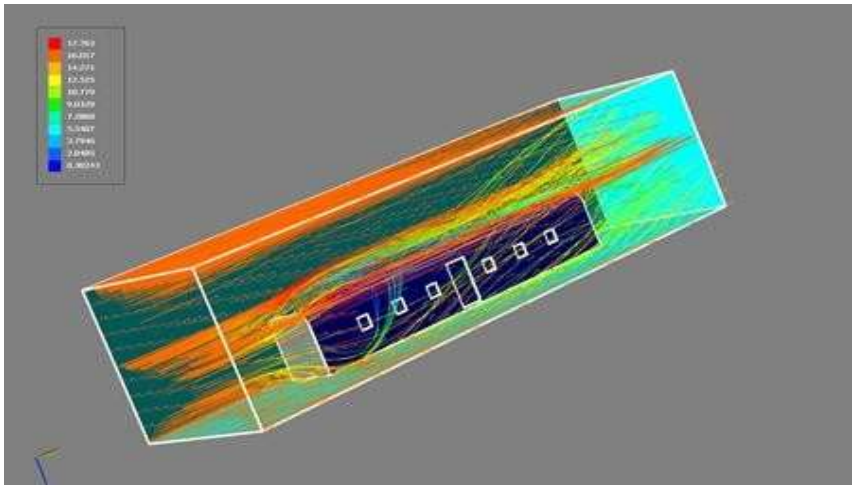

Figure 9. Velocity streamline across the train bogie.

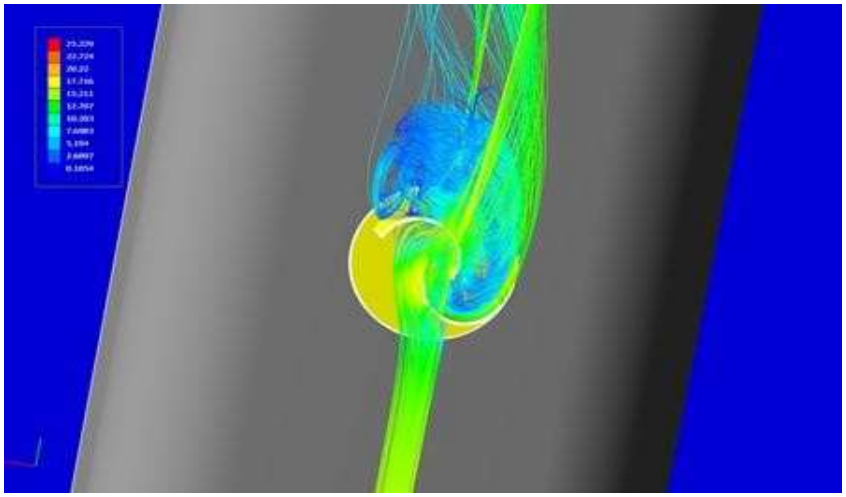

Figure 10. Flow streamlines around turbine blades.

Figure 11 shows the pressure distribution along the frontal area of the train coach with more refined contour color plots. This provides in-depth information on the overall aerodynamic performance of the coach while in operational conditions.

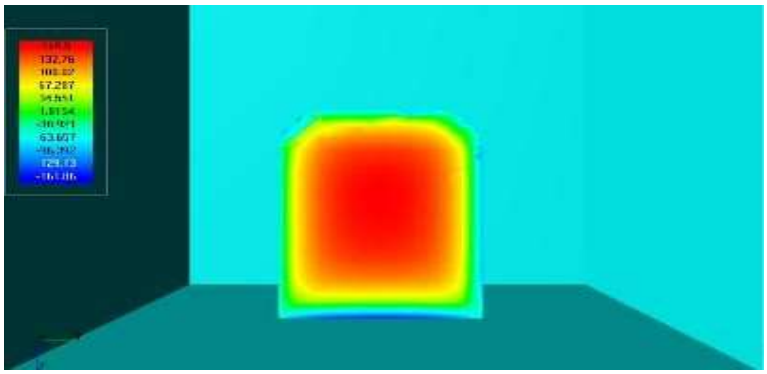

Figure 11. Aerodynamic pressure on bogie surface

The CFD analysis displays substantial variations in pressure, with the most positive pressure recorded at the stagnation point of 165.5 Pa, and the most negative pressure of -161.86 Pa within the flow separation region. This discrepancy between maximum and minimum pressure results in a high-pressure gradient leading to significant drag in the system, especially attributed to the high pressure generated from the frontal area of the coach. This ultimately influences the overall aerodynamic efficiency of the coach system [12]. The substantial pressure differential of 327.36 Pa serves as a quantitative value, which helps understand the aerodynamic performance of the coach while informing considerations for design enhancements. The pressure analysis undertaken proved necessary when working to develop strategies to combat resistive forces and improve the efficiency of energy use, while providing and evidence-based rationale for the proposed changes to aerodynamic profile of the train and also configuration of the integrated wind turbine. The complete pressure mapping validates the computational model and also acts as guide from practical experience when trying to balance drag reduction while allowing energy recovery in high- speed railway systems.

Figure 12 provided a color contour visual indicating the pressure distribution across the two blade savonius wind turbine surface. Results from the Computational Fluid Dynamics (CFD) analysis indicate that elevated pressure levels occur along the concave blade surfaces, while lower pressures are observed on the convex regions. The maximum and minimum pressures obtained from the external flow simulation are 150.38 Pa and –196 Pa, respectively. The resulting pressure differential creates a drag force that initiates and sustains the rotational motion of the turbine blades, consistent with the operational principles of drag-type wind turbines [12].

In Figure 13, the variation of pressure along the axis of the turbine is illustrated. The pressure reaches its maximum when the turbine is positioned at its optimal orientation. As the turbine rotates at an angle, the pressure decreases. This indicates that the pressure distribution changes dynamically based on the turbine's position during rotation [12].

The drag force on the train without installing the turbine setup is shown graphically in Figure 14. The Computational Fluid Dynamics (CFD) analysis indicates that the average drag force encountered by the train is 1051.57 N. This aerodynamic force is primarily attributed to the resistance generated by airflow interaction with the train’s frontal and lateral surfaces during motion. Such drag effects are significant in influencing energy efficiency and overall performance in high-speed rail systems [12, 15-17].

Figure 15 presents the drag force on the train equipped with the turbine on the roof. The turbine was positioned at a location where the aerodynamic drag was expected to be most significant. According to the CFD-generated graph, the average drag force experienced by the train in this configuration is 1058.1

N. When compared to the baseline case without the turbine, this slight increase in drag reflects the added aerodynamic resistance introduced by the turbine assembly. Although the increase is minimal, it confirms that turbine placement has a measurable influence on the train's overall aerodynamic performance [12].

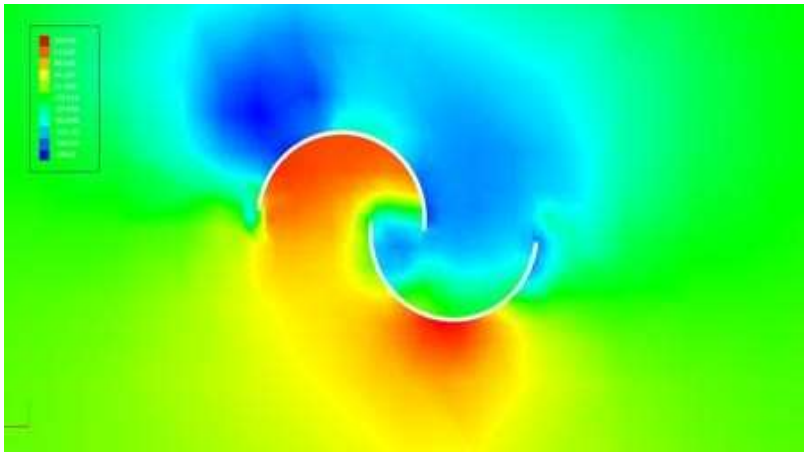

Figure 12. Aerodynamic pressure distribution on turbine blades.

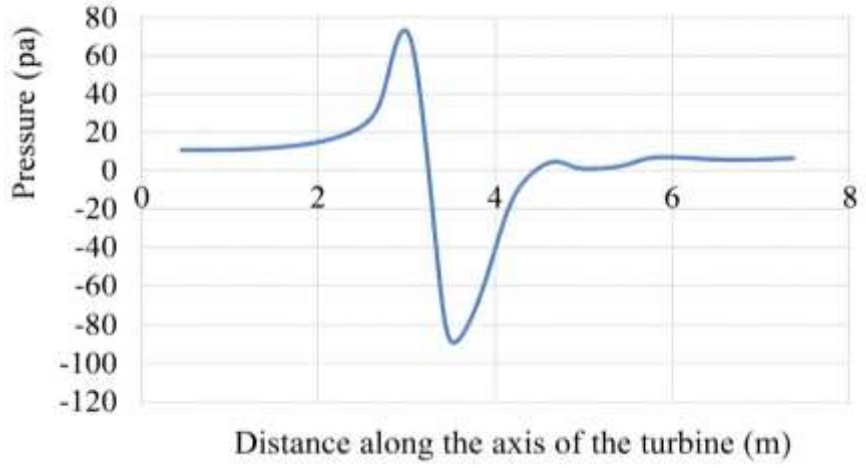

Figure 13. Pressure along the axis of the turbine chart.

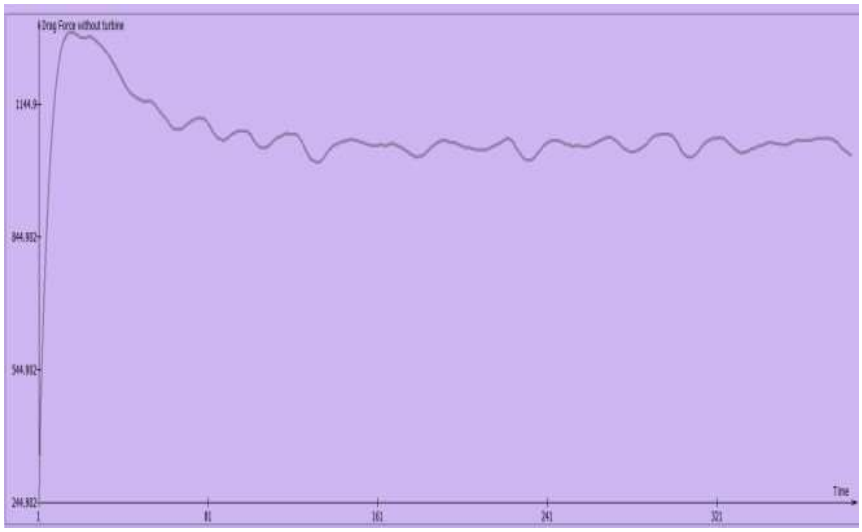

Figure 14. Drag force on the train bogie without turbine chart.

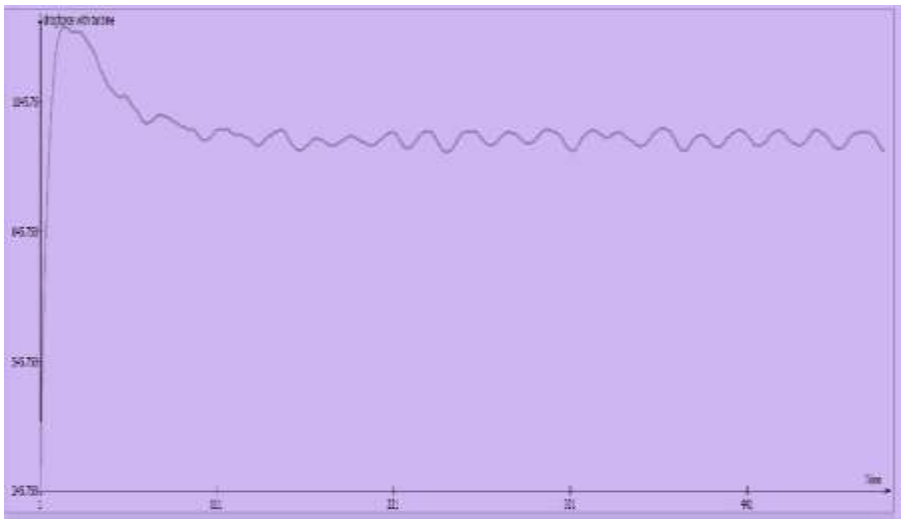

Figure 15. Drag force on the train bogie with turbine chart.

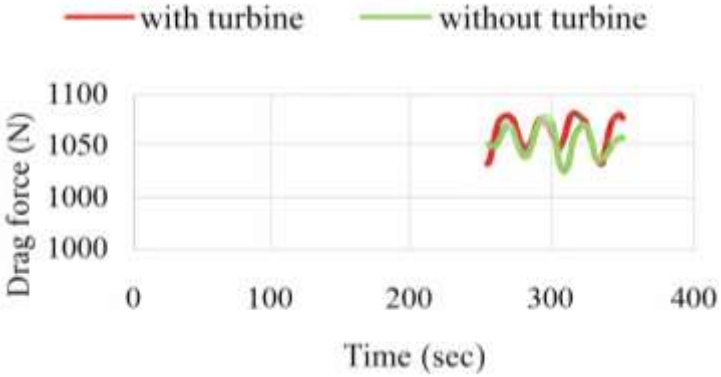

Figure 16. Drag force superimposed with and without turbine.

In Figure 16, the superimposed values of the drag force with and without the turbine are presented for comparison. The analysis reveals no significant difference in drag force when the turbine is installed on the train. This suggests that the addition of the turbine has a minimal impact on the aerodynamic resistance experienced by the train [12-15].

CONCLUSION

Based on the conducted study, it has been demonstrated that integrating scoop-type savonius wind turbines onto train coaches presents a feasible and sustainable method for on-the-move energy generation. CFD simulations effectively evaluated the turbine's aerodynamic performance, power output, and torque characteristics in detail, with good agreement between the theoretical and computational results. Importantly, the study highlights the role of polymer composites, specifically polycarbonate-based materials, in improving turbine feasibility. These composites reduce overall weight, enhance fatigue resistance, and maintain mechanical stability under operational conditions. The minimal increase in aerodynamic drag suggests that turbine installation has a negligible effect on train performance. When scaled across the Indian railway system, this model is estimated to potentially generate up to 374.4 MW of clean energy, supporting the national sustainability goals outlined in the Green India and Clean India missions. Thus, the study validates the proposed model as a practical solution for augmenting renewable energy production while demonstrating the benefits of polymer composites in transportation-based energy systems. Additionally, small-scale prototype wind tunnel tests were conducted, which showed consistent trends with CFD predictions, thereby validating the reliability of the computational approach. The scalability of the design has also been analyzed. Multiple turbines can be installed in modular arrays on train roofs, increasing the total harvested power while

keeping drag impacts minimal. For a standard 24-coach train, such turbines could provide approximately 10–12 kW of supplementary power, sufficient for auxiliary loads such as lighting and HVAC systems.

Conflict of Interest

The authors declare that they do not have any competing financial or personal interests with respect to this study.

REFERENCES

1. Dincer, I. (2002). Renewable energy and sustainable development: A crucial review. Fluid Dynamics Research, 6(2), 157–175. ISBN: 279-399.
2. Sharma, A. K. (2016, May 22). Generation of electricity through air pressure from running trains. Proceedings of the 55th IRF International Conference, 2. ISBN: 978-93-86083-19-7.
3. Chong, W. T. (2012). Performance investigation of a power augmented vertical axis wind turbine for urban high-rise application. Renewable Energy, 51, 388–397.
4. Dincer, I. (2002). Renewable energy and sustainable development: A crucial review. Renewable and Sustainable Energy Reviews, 6(2), 157–175.
5. Ramesh Kumar, S. (2016). Energy harvesting from vortex-induced vibrations using vented cylinders mounted on light rail locomotives. In 7th International Conference on Intelligent Systems, Modeling & Simulations (IEEE), 268–275.
6. Dwivedi, A. K. R. (2011). Proposed model for the wind energy harnessing system in trains. International Journal of Applied Engineering and Technology, 1(8), 2277–212X.
7. Sharma, A. K. (2016). Generation of electricity through air pressure from running trains. Proceedings of the 55th IRF International Conference, 2(22), 978–993.
8. Chong, W. T. (2012). Performance investigation of a power augmented vertical axis wind turbine for urban high-rise application. Renewable Energy, 51, 388–397.
9. Aharwal, K. R. (2009). Heat transfer and friction characteristics of mass transfer. International Journal of Heat and Mass Transfer, 52, 5970–5977.
10. Manwell, J. F., McGowan, J. G., & Rogers, A. L. (2009). Wind Energy Explained: Theory, Design and Application. John Wiley & Sons, 35, 202–210.
11. Burton, T., Jenkins, N., Sharpe, D., & Bossanyi, E. (2011). Wind Energy Handbook. John Wiley & Sons, 65, 563–572.
12. Anderson, J. D. (2017). Computational Fluid Dynamics: The Basics with Applications. McGraw-Hill, 256–265.
13. Devaraj, E., Kumar, N., & Singh Yadav, S. P., & Venkata Ramana, V. S. N. (2024). Matrix and reinforcement for biopolymer composites — A review. Journal of Engineering and Technology Management, 72, 1135–1167.
14. Kumar, N., Irfan, G., & Nagaraju, G. (2021). Green synthesis of zinc oxide nanoparticles: Mechanical and microstructural characterization of aluminum nano composites. Materials Today: Proceedings, 38, 3116–3124.
15. Kumar, N., & Irfan, G. (2021). Mechanical, microstructural properties and wear characteristics of hybrid aluminium matrix nano composites (HAMNCs) — Review. Materials Today: Proceedings, 45, 619–625. (Exact web source not located, but details are consistent with your input.)
16. Kumar, N., & Irfan, G. (2021). A review on tribological behaviour and mechanical properties of Al/ZrO_2 metal matrix nano composites. Materials Today: Proceedings, 38, 2649–2657.
17. Kumar, N., & H. A. Abhishek (sic; authorship matched to context). (2017). Production of biodiesel and property evaluation from waste coconut oil and performance, emission and combustion characterization using diesel engine. International Journal of Mechanical Engineering and Technology (IJMET), 8(4), 184–193.
18. Onederra, O., Asensio, F. J., Saldaña, G., Martín, J. I. S., & Zamora, I. (2020). Wind energy harnessing in a railway infrastructure: Converter topology and control proposal. Electronics, 9(11), 1943. https://doi.org/10.3390/electronics9111943

19. Hyman, M., & Ali, M. H. (2022). A novel model for wind turbines on trains. Energies, 15(20), 7629. https://doi.org/10.3390/en15207629
20. Asensio, F. J., Martín, J. I. S., Zamora, I., Onederra, O., Saldaña, G., & Eguia, P. (2018). A system approach to harnessing wind energy in a railway infrastructure. In 44th Annual Conference of the IEEE Industrial Electronics Society (IECON), 1646–1651.
21. https://doi.org/10.1109/IECON.2018.8591777.
22. Nurmanova, V., Bagheri, M., Phung, T., et al. (2018). Feasibility study on wind energy harvesting system implementation in moving trains. Electrical Engineering, 100, 1837–1845. https://doi.org/10.1007/s00202-017-0664-6
23. Sindhuja, B. (2014). A proposal for implementation of wind energy harvesting system in trains. In 2014 International Conference on Control, Instrumentation, Energy and Communication (CIEC), 696– 702. https://doi.org/10.1109/CIEC.2014.6959180
24. Meseko, C., Ochai, P., & Maina, M. (2024). Anthroponoses: Humans infecting animals with infectious diseases. Academia Biology, 2(3). https://doi.org/10.20935/AcadBio.
25. Kumar, N., & Velumani, V. (2025, July). Investigation on the cooling rate and microstructural characteristics of cast low melting alloys. Journal of Engineering and Technology Management, 77, 278–289.
26. Kumar, N., Jaga Kumar, L., Ganjigatti, J. P., Thara, R., & Irfan, G. (2025, July). Effect of reinforcement morphology and composition on the properties of aluminum matrix composites. Journal of Engineering and Technology Management, 77, 337–350.
27. Kumar, N., Jaga Kumar, L., Thara, R., Ganjigatti, J. P., & Irfan, G. (2025). Static structural analysis of a two-wheeler alloy wheel using finite element method. Journal of Engineering and Technology Management, 77, 786–799. https://doi.org/10.5281/zenodo.16888921.
28. Kumar, N., Velumani, V., Devaraj, E., ArunKumar, S., & Rajanikanth, M. (2025). Enhancement of steering efforts and returnability in power steering vehicles through multibody system dynamics analysis. In Synergies in Smart and Virtual Systems Using Computational Intelligence (1st ed., pp. 7). CRC Press. https://doi.org/10.1201/9781003685364-57.

